

1 **Domestic Well Capture Zone and Influence of the Gravel Pack Length**

2 Judith E. Horn and Thomas Harter*

3 Department of Land, Air, and Water Resources

4 University of California

5 Davis, CA 95616-8629

- 6 • (corresponding author; ThHarter@ucdavis.edu; 530-752-2709)

7
8 Accepted for publication in the journal “Ground Water”, September 2008

9
10 **Abstract**

11 Domestic wells in North America and elsewhere are typically constructed at relatively shallow
12 depths and with the sand or gravel pack extending far above the intake screen of the well (shallow
13 well seal). The source areas of these domestic wells and the effect of an extended gravel pack on the
14 source area are typically unknown and few resources exist for estimating these. In this paper, we use
15 detailed, high-resolution groundwater modeling to estimate the capture zone (source area) of a
16 typical domestic well located in an alluvial aquifer. Results for a wide range of aquifer and gravel
17 pack hydraulic conductivities are compared to a simple analytical model. Correction factors for the
18 analytical model are computed based on statistical regression of the numerical results against the
19 analytical model. This tool can be applied to estimate the source area of a domestic well for a wide
20 range of conditions. We show that an extended gravel pack above the well screen may contribute
21 significantly to the overall inflow to a domestic well, especially in less permeable aquifers, where
22 that contribution may range from 20% to 50%; and that an extended gravel pack may lead to a
23 significantly elongated capture zone, in some instances nearly doubling the length of the capture

24 zone. Extending the gravel pack much above the intake screen therefore significantly increases the
25 vulnerability of the water source.

26

27 **Introduction**

28 Most households in rural areas of the United States, outside the service area of incorporated cities,
29 rely on domestic wells for their water supply (McCray 2005, U.S. EPA 1997). And many of these
30 domestic wells are constructed with a well-screen at depth and a sand or gravel pack that extends
31 upward to the mandatory minimum depth of the well seal, which is dictated by local and state
32 guidelines. A question commonly asked by homeowners is: Where does our water come from? The
33 capture zones (also referred to as the source area or recharge area) of domestic wells are rarely
34 determined. Attention has instead focused on public supply wells and their capture zones as these are
35 regulated through U.S. EPA's source water protection program. Domestic wells, typically serving a
36 single family, are often constructed to relatively shallow depths when compared to public or
37 municipal water supply wells (Burow et al. 2004).

38

39 Methods for delineating well capture zones range from very simple to very complex. In general, the
40 various approaches fall into four categories (Harter, 2008):

- 41 1. Geometric or graphical methods involve the use of a pre-determined fixed radius without any
42 special consideration of the flow system, or the use of simplified shapes that have been pre-
43 calculated for a range of pumping and aquifer conditions.
- 44 2. Analytical methods allow calculation of distances for protection zones using equations that can be
45 solved using a hand calculator or microcomputer spreadsheet program.

46 3. Hydrogeologic mapping involves identifying the recharge zone and the source zone based on
47 geomorphic, geologic, hydrologic, and hydrochemical characteristics of an aquifer.

48 4. Computer modeling methods involve devising, calibrating, and applying complex analytical or
49 numerical models that simulate groundwater flow and contaminant transport processes.

50 The long-term average pumping rate of domestic wells typically ranges from less than 4 L/min [1
51 gallon/min] to 20 L/min [5 gallon/min]. Using the graphical method employed by California's
52 Drinking Water Source Assessment and Protection (DWSAP) Program (California DHS, 1999), for
53 example, the default source area of a domestic well pumping 1,233.5 m³/year (1 acre-foot per year,
54 the typical annual consumption of a U.S. single family household) is a circle with a radius of 15 m
55 (~50 ft) for areal recharge of 450 mm/year (typical for very humid areas or rural residences in semi-
56 arid areas surrounded by irrigated lawn and fields) or with a radius of 31 m (~100ft) at a recharge
57 rate of 100 mm/year (typical of many semi-arid regions). This simple geometric approach neglects
58 the effects of the regional groundwater flow on the capture zone of a domestic well.

59

60 On the other hand, where regional groundwater flow is dominant and local recharge is negligible, the
61 capture zone of a domestic well can also be easily computed if the well fully penetrates the aquifer
62 system or does not strongly affect regional groundwater flow. The width, w , of the capture zone of a
63 domestic well is then obtained by simple mass balance (Todd 1980):

64
$$w = Q / (T * i) \quad (1)$$

65 where Q is the pumping rate, T is the aquifer transmissivity, and i is the regional hydraulic gradient.

66 For example, at a relatively low transmissivity, T , of 10 m²/d, a regional groundwater gradient of
67 0.5% and a pumping rate of 1,233 m³/year, the width of the capture zone is approximately 60 m

68 (~200 feet). At values of T typical for productive aquifers, the width of the capture zone is often on
69 the order of 1 m - 10 m (~ 3 feet - ~30 feet) or even less.

70

71 Both, the geometric approach and equation (1) above provide simple approximations for extremely
72 idealized conditions. Here, our objective is to determine the capture zone of a domestic well with a
73 sand or gravel pack, completed in an unconfined aquifer, where both, recharge and regional
74 groundwater flow are significant. We use high-resolution computer simulations to determine the
75 source area and to explicitly determine the influence of the gravel pack on the well capture zone. For
76 reference, we compare those to a simple analytical model of the capture zone for a low-producing
77 well in an unconfined aquifer with recharge. Our study's focus is on rural domestic wells in irrigated
78 agricultural regions, e.g., of the Southwestern United States, where significant recharge is due to
79 irrigation return flows and much of the groundwater production is for irrigation purposes. Our
80 findings have general implications that are independent of this particular climate scenario.

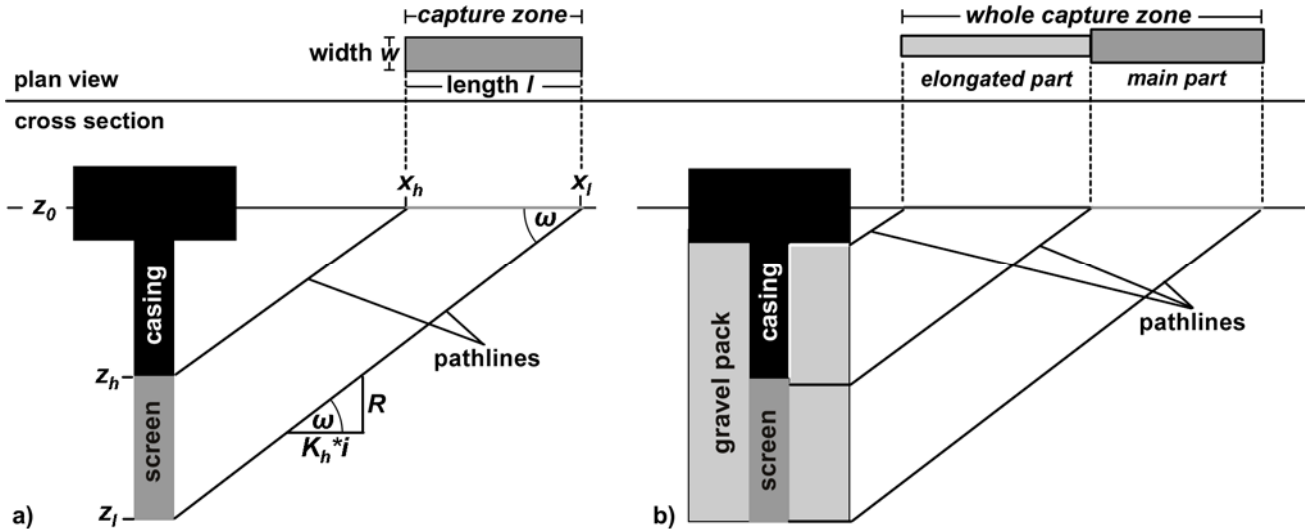
81

82 **Conceptual Framework**

83 Domestic wells in rural areas are assumed to be completed near the uppermost portion of a regional
84 aquifer system. Furthermore, we assume that a significant downward gradient exists in the regional
85 aquifer system due to recharge at the water table and due to significant groundwater production
86 (mostly for irrigation) from the deeper portions of the aquifer system (e.g., Belitz and Phillips,
87 1995). Burow et al. (2004), for example, report typical recharge rates in irrigated areas in the San
88 Joaquin Valley, California, to be on the order of 550 – 750 mm/a with the majority of recharge
89 originating from irrigation return flows. For simplicity, regional groundwater flow is considered to
90 be uniform around the source area of the domestic well and at steady-state. The superposition of
91 regional groundwater flow with the downward gradient induced by water table recharge and deeper

92 groundwater production yields a groundwater flow field that is vertically inclined relative to the
 93 slope of the water table (**Figure 1**).

94



95

96 **Figure 1:** Conceptual framework of groundwater flow towards a partially penetrating domestic well
 97 (a) without and (b) with a gravel pack that extends for several meters to several tens of meters above
 98 the well screen. Top: plan view, bottom: cross-sectional view. Regional groundwater flow is from
 99 right to left with a vertical flow component controlled by uniform recharge at the top and aquifer
 100 pumping from large production wells dispersed in the deep part of the aquifer below. The aquifer
 101 bottom is assumed to be much deeper than the typical depth of the (relatively shallow) domestic
 102 well; l : length, w : width. All other symbols: see text for details.

103

104 A simple method to compute the approximate source area size and location is available, if we
 105 neglect the effects of the gravel pack and the effects of domestic well pumping, Q , on the local
 106 groundwater flow field. Then, the source area location is obtained from the length and depth of the
 107 domestic well screen, and from the angle, ω , of groundwater flow relative to the slope of the water
 108 table (**Figure 1a**):

109

$$x_h = x_w + \frac{z_0 - z_h}{\tan \omega} \quad (2)$$

110

$$x_l = x_w + \frac{z_0 - z_l}{\tan \omega} \quad (3)$$

111

$$l_{theo} = x_l - x_h \quad (4)$$

112
$$A_{theo} = Q/R \quad (5)$$

113
$$w_{theo} = \frac{A_{theo}}{l_{theo}} \quad (6)$$

114 where x_w is the location of the well (along the regional groundwater gradient), x_h is the location of
115 the downgradient edge of the recharge (source) area, x_l is the location of the upgradient edge of the
116 recharge area, z_0 is the elevation of the water table, z_h is the elevation of the top the well screen, z_l is
117 the elevation of the bottom of the well screen (**Figure 1a**), l_{theo} , w_{theo} , A_{theo} are the theoretical length,
118 width, and area of the recharge zone, and:

119
$$\tan \omega = R / (K_h * i) \quad (7)$$

120 where R is the uniform recharge rate, K_h is aquifer hydraulic conductivity, and i is the regional
121 hydraulic gradient. Equations (2) – (7) provide a simple analytical model to determine the capture
122 zone of a domestic well in an unconfined aquifer with uniform flow, recharge, and deep production.

123

124 To account for the influence of domestic well pumping on the local groundwater flow system around
125 the well and to account specifically for the influence of the gravel pack on the recharge area (**Figure**
126 **1b**), we constructed a numerical model, described in the next section.

127

128 **Modeling Methods**

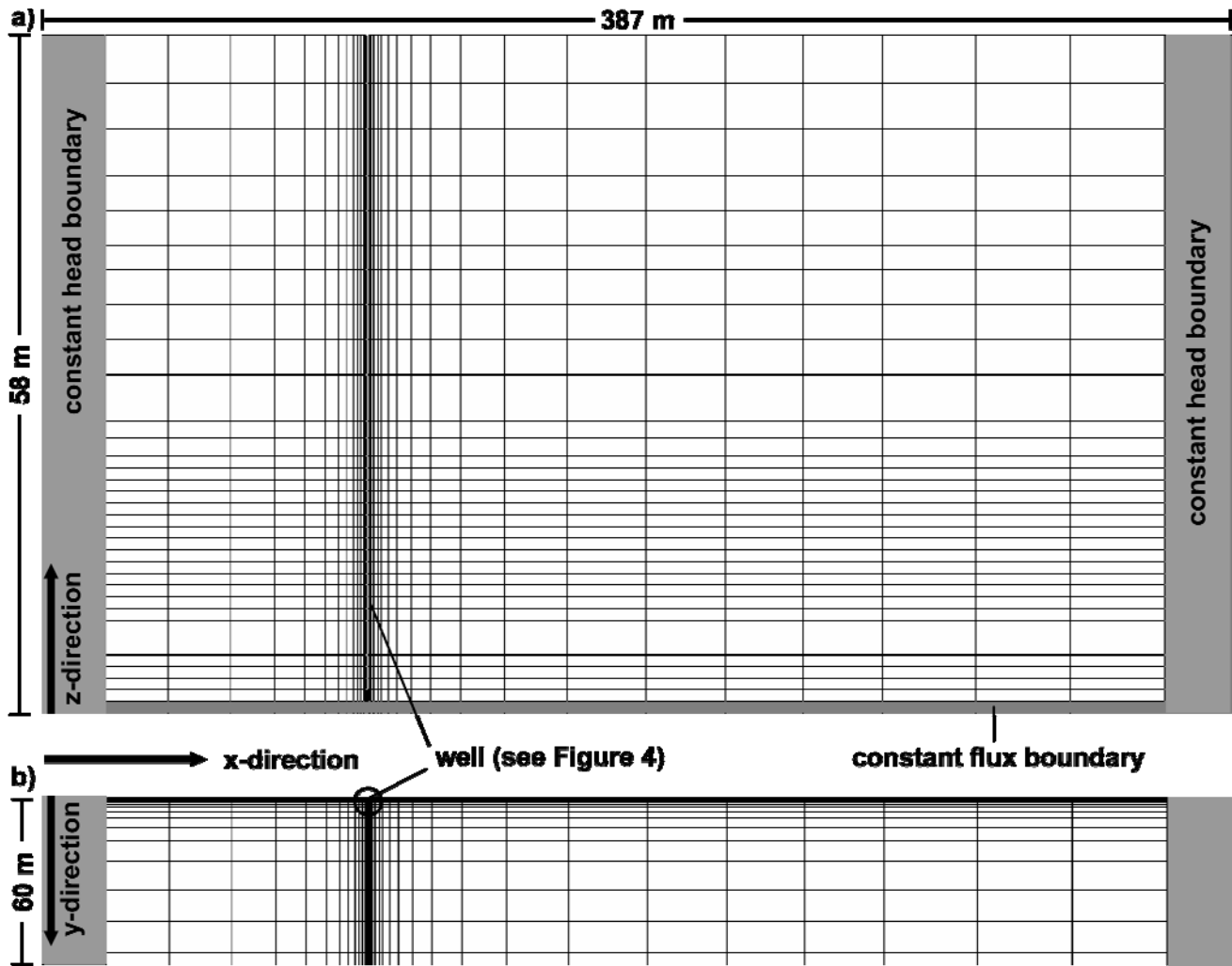
129 The capture zone of a domestic well with a gravel pack is computed for a fully three-dimensional
130 steady-state groundwater flow field. The steady-state head and flux distribution are computed using
131 the MODFLOW groundwater flow model (McDonald and Harbaugh 1988). The capture zone
132 corresponding to a particular groundwater flow solution is delineated using the backward particle
133 tracking model MODPATH (Pollock 1994).

134

135 Briefly, MODFLOW solves the steady-state groundwater flow equation

136
$$\nabla \underline{\underline{K}} \nabla h = 0 \quad (8)$$

137 where h is the hydraulic head, by using a fully three-dimensional block-centered finite difference
138 scheme for the user-specified boundary conditions, \mathbf{K} is the hydraulic conductivity tensor. In the
139 following simulations pumping induces only a small drawdown of the piezometric surface, so the
140 linear flow model (8) is sufficiently accurate for our purposes. We effectively invoke the Dupuit
141 assumption equivalent to the MODFLOW “unconfined layer” algorithm. There, the unconfined layer
142 thicknesses are set constant and only updated iteratively. From the hydraulic head solution,
143 MODFLOW also computes the flux, q , across each of the six faces of each finite difference cell in
144 the modeling domain. The flux solution becomes input to MODPATH, which computes backward
145 particle travel paths given the linear groundwater velocity, $v = q/n$, where n is the effective porosity,
146 across each finite difference cell face. Starting locations for backward particle paths are user-defined.
147 MODPATH uses a semi-analytical linear interpolation scheme to compute a spatially continuous
148 particle path (Pollock 1994).



149
150
151
152
153
154
155

Figure 2: Model grid in (a) cross-sectional view at $y = 0$ (Vertical exaggeration = $4.2x$) and (b) in plan view. Due to the symmetry of the flow field, the model domain simulates only half of a well and half of the capture zone. The well and gravel pack are very finely discretized. A close-up view of the model around the well screen is shown in Figure 4.

156 Our modeling domain is a finite difference grid with 141,750 cells of which 137,937 are active. The
157 modeling domain is 58 m high, 387.23 m long and 59.695 m wide and consists of 45 rows, 90
158 columns, and 35 layers. The modeling domain takes advantage of the symmetry in the well flow
159 field, which is symmetric across the x -axis (mean flow direction) centered on the domestic well ($y =$
160 0, see below). The model is therefore designed to model only one-half of the well capture zone
161 (**Figure 2**). The second half of the well-capture zone mirrors the first half. Grid spacing is non-

162 uniform in both the vertical and horizontal direction. Vertical grid spacing varies from 1 m at the
163 elevation of the well screen to 4 m elsewhere (**Figures 2, 3**). Horizontal grid-spacing varies from
164 0.01 m near the well and in the gravel pack to nearly 20 m near the model boundaries. The
165 horizontal increase in cell-size between adjacent rows or columns of the finite-difference grid is set
166 to not exceed 50 % of its width.

167

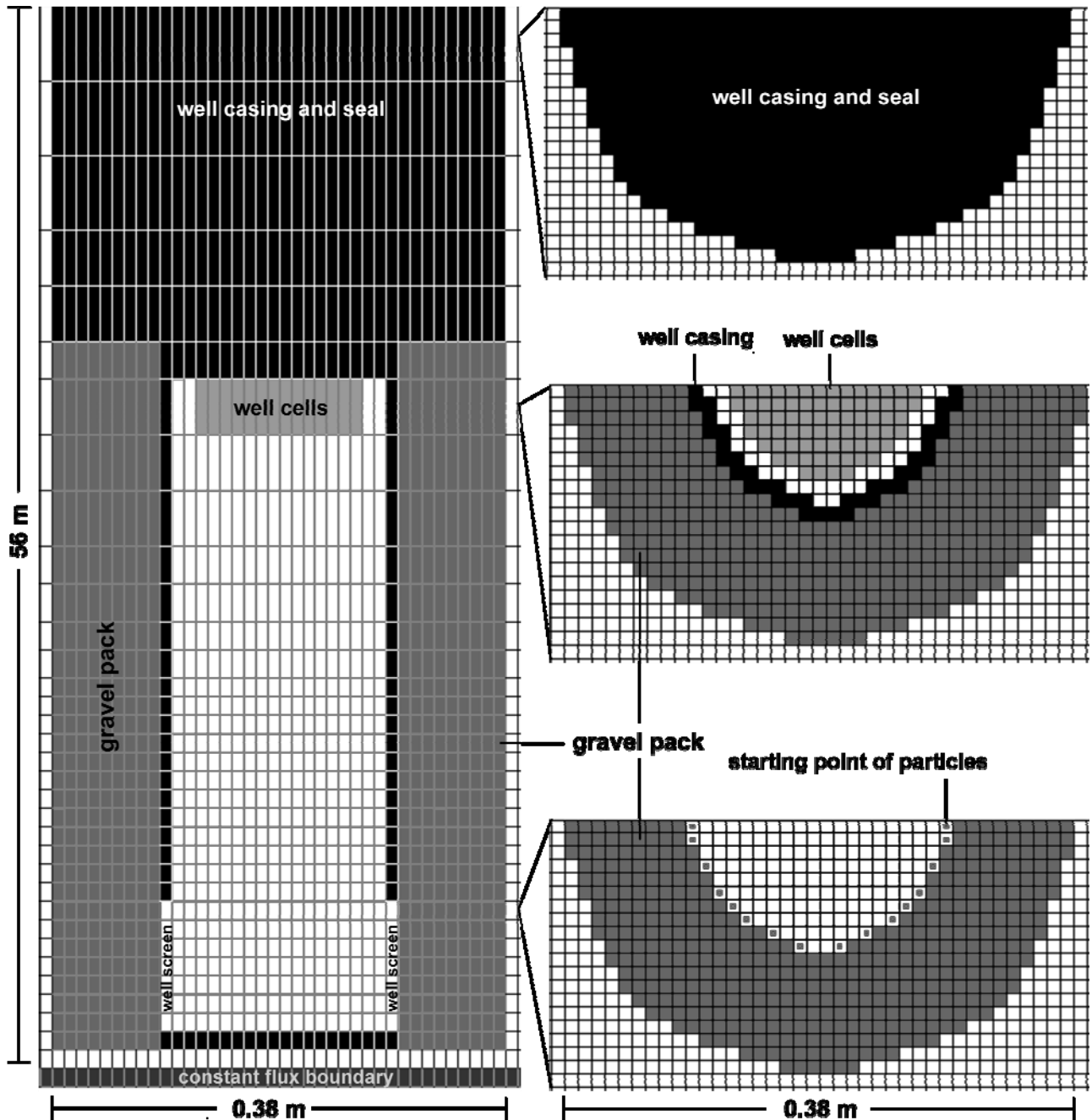
168 The hydraulic gradient along the x-axis is produced by defining a constant head boundary of 58.00
169 m to the exterior block of cells at the upgradient vertical side of the model and a constant head of
170 57.61 m at the downgradient vertical side of the model (**Figure 2**). This is equivalent to a hydraulic
171 gradient of 0.0018, which is typical for the study area. The other two vertical planes of the model are
172 assigned no-flow boundary condition: the vertical plane adjacent to the well half is a symmetry
173 plane. The vertical plane opposite of the half well is at sufficient distance to the well that the local
174 effect of pumping on the groundwater flow field can be neglected and flow is parallel to regional
175 groundwater flow. The average (steady-state) recharge rate is set to 0.669 m/year, a value typical for
176 semi-arid, irrigated agricultural regions such as the Modesto Area, San Joaquin Valley, California.
177 The bottom of the model domain is considered permeable and open to the regional aquifer system
178 below. It is assigned a uniform constant (downward) flux boundary condition, with total outflow
179 across the bottom boundary set equal to the difference between the total recharge inflow at the top
180 and the well outflow rate. In this way we implicitly enhance our model to greater aquifer depths. In
181 the Modesto Area large irrigation wells up to a depth of almost 370 m below land surface pump
182 large amounts of water and produce a vertical flow component, even through a confining clay unit
183 above the irrigation wells (Burow et al. 2004).

184

185 The well construction was chosen to be representative of domestic well construction in the San
186 Joaquin Valley, California (e.g., Burow et al., 2004). The model well has a total depth of 56 m below
187 the water table. A seal to 18 m below the water table overlies a 30 m long gravel pack around a
188 blank well casing. The casing has a diameter of 0.2 m. The perforated well screen is located at 48 m
189 to 55 m below the water table, followed by a conceptual well sump from 55 m – 56 m. Casing and
190 screen are surrounded by a 0.09 m thick gravel pack. The total borehole diameter is 0.38 m. Due to
191 the relatively low pumping rate, the well-loss and skin effect are assumed to be negligible. Inflow
192 along the screen is computed by the model and non-uniformly distributed.

193

194 The grouted well seal above the gravel pack and the well casing are modeled as “no-flow” cells
195 (black cells in **Figure 3**). The pump is simulated by 74 “well” cells inside the casing. They are
196 located significantly above the top of the screen, opposite of the well seal bottom, which creates an
197 upward flow inside the screen and casing. The MODFLOW “well” package is used to simulate the
198 pump cells (light-grey cells in **Figure 3**). The total pumping rate of the domestic well is 3.5 m³/d,
199 half of which is uniformly distributed across the individual “well” cells at the top of the casing.
200 Flow inside the model well casing was modeled by approximating the flow with eq. (8) using very
201 high hydraulic conductivity. The gravel pack (grey cells in **Figure 3**) is modeled by choosing a
202 separate hydraulic conductivity that is higher than that of the surrounding aquifer and ranges
203 between 50 and 1000 [m/d] (**Table 1**). Modeling the pump inside the well allows the model to
204 properly distribute the flow across the well screen, with screen inflow highest near the top of the
205 screen and lowest at the bottom of the screen.



206
 207
 208
 209
 210
 211
 212
 213
 214

Figure 3: Model well configuration and grid discretization around the well. Left: Cross-section at the model boundary ($y = 0$). Right: Plan view at the land surface (right top), at the top layer of the casing containing the well cells (right center), and at the screen elevation (right bottom). Black cells: casing and well seal (impermeable). Grey cells: gravel pack. Dark grey cells: constant flux boundary cells at the model bottom. Grey dots in the lower left panel indicate the starting location for backward particle tracking.

215 The hydraulic conductivity, K_h , is assumed to be isotropic in the horizontal plane, while the vertical
 216 aquifer hydraulic conductivity, K_v , is lower, as typically observed in alluvial aquifers (e.g., Phillips
 217 et al., 2007). Two representative anisotropy ratios, $K_h/K_v = 5$ and 2, were chosen to bracket a
 218 representative range typically found in alluvial aquifers (*ibid.*). The gravel pack itself is assumed to
 219 have a completely isotropic hydraulic conductivity, K_g , that is larger than K_h . For illustration and
 220 application purposes, we modeled well capture zones for a wide range of representative values for
 221 the horizontal hydraulic conductivity, K_h , and the gravel pack hydraulic conductivity, K_g , and for two
 222 anisotropy ratios (**Table 1**).

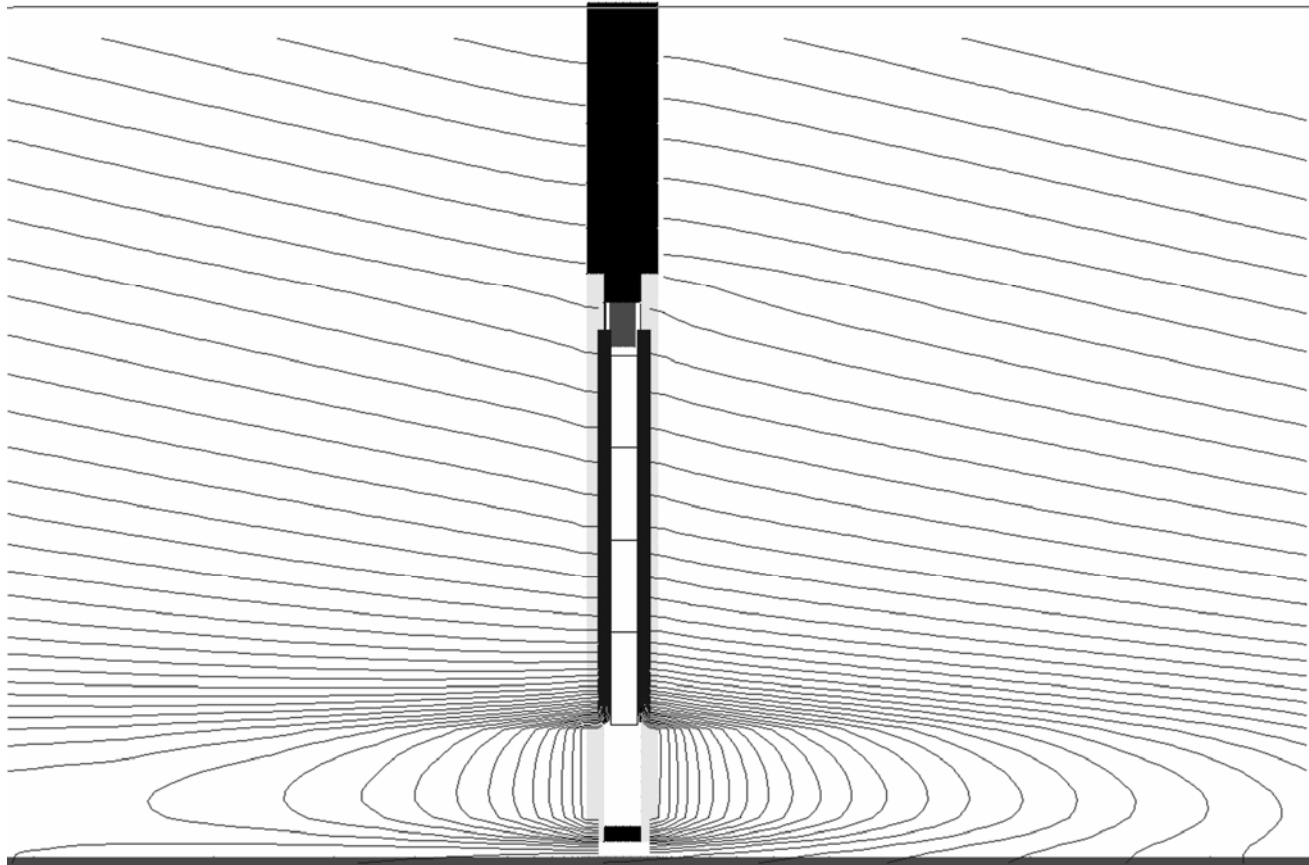
K_h	K_v	K_g
1	0.2	50, 125, 250, 500, 750, 1000
1	0.5	50, 125, 250, 500, 750, 1000
3	0.6	50, 125, 250, 500, 750, 1000
3	1.5	50, 125, 250, 500, 750, 1000
5	1	50, 125, 250, 500, 750, 1000
5	2.5	50, 125, 250, 500, 750, 1000
10	2	50, 125, 250, 500, 750, 1000
10	5	50, 125, 250, 500, 750, 1000
30	6	50, 125, 250, 500, 750, 1000
30	15	50, 125, 250, 500, 750, 1000
100	20	125, 250, 500, 750, 1000
100	50	125, 250, 500, 750, 1000
300	60	500, 750, 1000
300	150	500, 750, 1000

223
 224 **Table 1:** Model configurations with various
 225 combinations of the horizontal hydraulic
 226 conductivity, K_h , the vertical hydraulic
 227 conductivity, K_v , and the gravel pack hydraulic
 228 conductivity, K_g . All values are in units of
 229 [m/d].
 230

231 **Results**

232 Head contour configurations in the aquifer around the domestic well are highly dependent on the
 233 aquifer and gravel pack hydraulic conductivities. Cross-sectional head contour lines along the

234 regional flowpath are vertical under strictly regional flow with no recharge and no pumping. As
235 expected from the analytical model above, the modeled contours deviate from the vertical due to the
236 vertical flow component imposed by the recharge at the top of the model area and the regional
237 pumping below the modeled zone. Contour lines increasingly deviate from the vertical alignment
238 with smaller and smaller ratios of K_h / R (**Figure 4**). In addition, in aquifers with relatively low
239 hydraulic conductivity, the domestic well creates a distinct zone of local influence in the aquifer
240 around the well screen, whereas the influence is minimal in the highly permeable aquifer. The
241 anisotropy of the aquifer hydraulic conductivity creates significant flow zonation: much of the
242 impact of domestic well pumping on the pressure field is seen at the elevation of the well screens,
243 especially for those cases with the higher aquifer anisotropy. Another distinct horizontal zone is
244 created by the top of the gravel pack. The higher the gravel pack hydraulic conductivity (relative to
245 K_h), and the higher the aquifer anisotropy ratio, K_h/K_v , the more pronounced is the effect that the
246 transition between the top of the gravel pack and the annular seal has on the head contour lines (e.g.,
247 **Figure 4**). Inflow to the well varies non-uniformly along the screen. It is highest near the top of the
248 screen, which is nearest to the pump intake inside the well-casing. The difference between the screen
249 inflow at the top (layer 26) and the screen inflow near the bottom (usually in layer 31 just above the
250 bottom of the layer) varies from approximately 45% for highly permeable aquifers to more than
251 100% for very low permeable aquifers with very high gravel pack K_g . This is consistent with
252 analytical models (Nahrgang, 1954; Garg and Lal, 1971) and with field observations on large
253 production wells (VonHofe and Helweg, 1998).

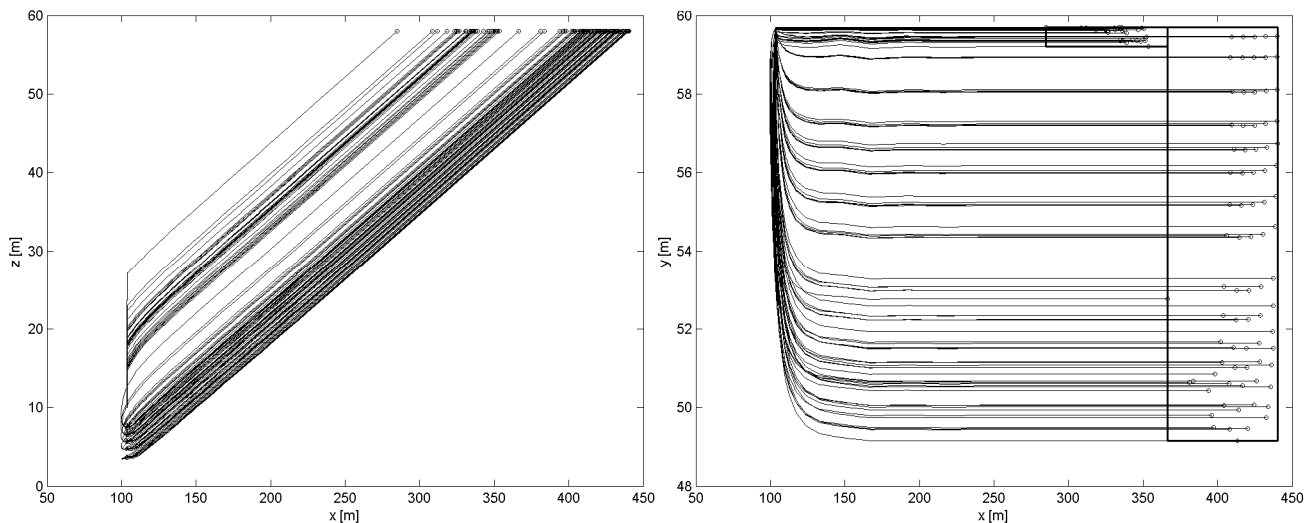


254
 255 **Figure 4:** Head contour lines around the well for a conductivity of 10 m/d, an anisotropy ratio of 2,
 256 and hydraulic gravel pack conductivity of 750 m/d. The heads depend on the conductivity of the
 257 aquifer, the anisotropy and the relative difference in the conductivities between gravel pack and
 258 aquifer. Horizontal dimension is 7 m, vertical dimension is 58 m. Due to the horizontal exaggeration
 259 (12.4x) the inclination of the head contours in the regional flow field (near top of the cross-section
 260 appears nearly horizontal although it is actually nearly vertical.
 261

262 Corresponding to the head field, pathlines in low hydraulic conductivity aquifers are significantly
 263 steeper and the capture zone is much closer to the well-head than in an aquifer with high hydraulic
 264 conductivity (**Figure 5**). For $K_h \geq 10$ m/day, the modeled pathlines are in fact sufficiently flat that
 265 the source area is outside the model area. In those simulations, we computed the pathlines outside
 266 the numerical modeling area by analytically calculating the extension of the pathlines to the water
 267 table using equation (7). Also, for model scenarios with hydraulic conductivities of 1, 3, and 5 m/d,
 268 the pathlines in the top aquifer layer were computed from eq. (7), because MODPATH computations
 269 in the top layer were subject to numerical error.

270

271 The source area of the domestic well has a distinct shape composed of two features: the main
272 capture zone, a relatively large and wide oval area, corresponding to pathlines that enter the annulus
273 of the well below the top of the well-screen for horizontal delivery into the well. At the
274 downgradient (well-facing) side of this main capture zone, we observe a narrow elongated capture
275 subzone that represents those pathlines that enter the gravel-pack of the well at some distance above
276 the well screen. These pathlines capture domestic water through the high permeability field of the
277 gravel pack above the well screen (**Figure 1b, Figure 5**). The greater the hydraulic conductivity
278 difference between gravel pack and aquifer, the higher is the relative downward flow in the upper
279 gravel pack, and the more MODPATH virtual water particles enter the well flowing through the
280 upper gravel pack. Moreover, the steeper the particle path gradient, the higher is the highest point of
281 entry into the gravel pack of pathlines that ultimately will be captured by the well. Thus, the gravel
282 pack, where it extends to elevations much higher than the well-screen, significantly extends the
283 length of the source area towards the well, albeit within a very narrow transverse range (**Figure 5**).

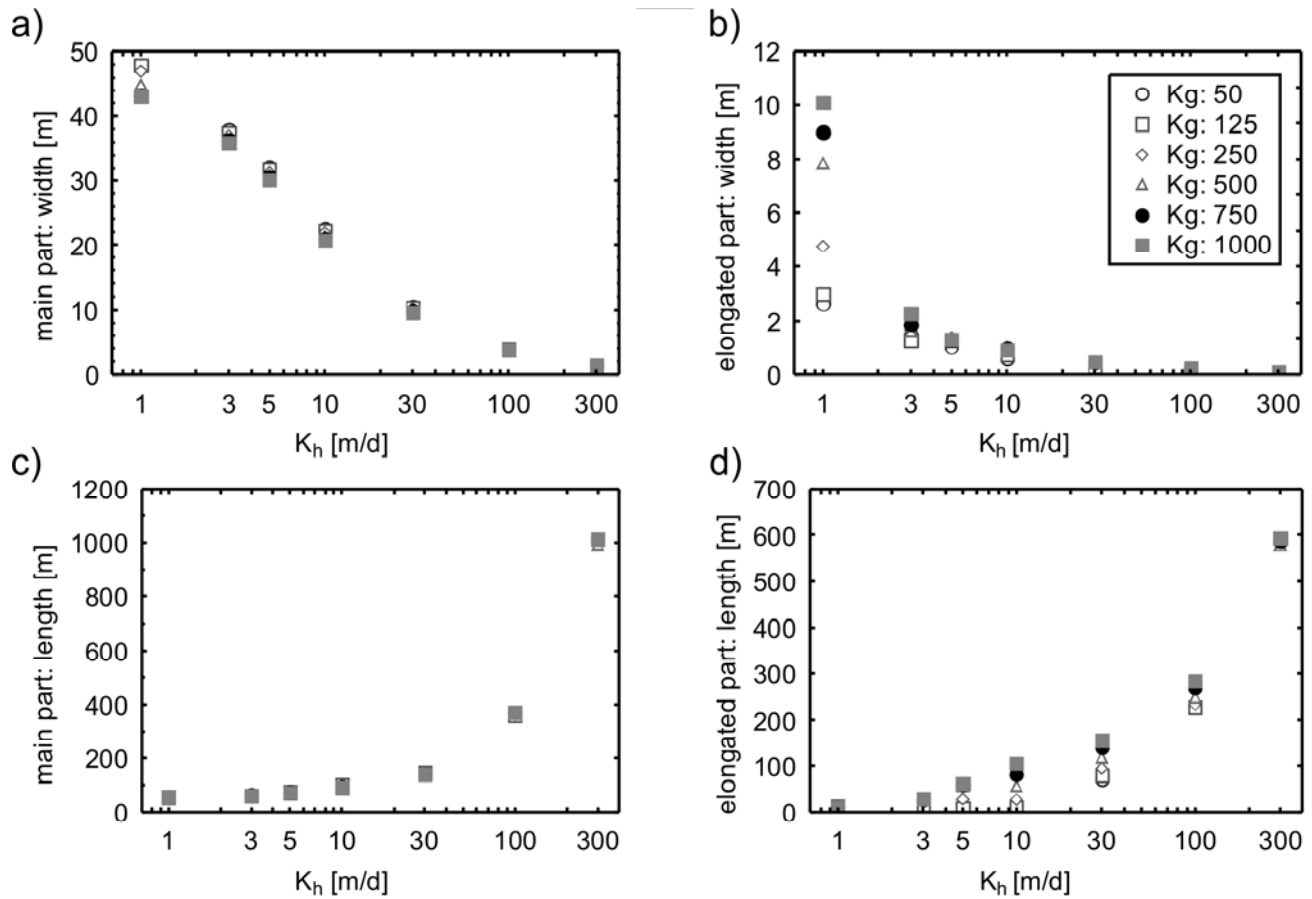


284

285 **Figure 5:** Pathlines in cross section (left) and plan view (half the well, right) with the elongated and
286 main capture zone parts for an aquifer conductivity of 10 m/d, an anisotropy ratio of 2, and gravel
287 pack conductivity of 750 m/d. Corresponding heads are shown in Figure 4.

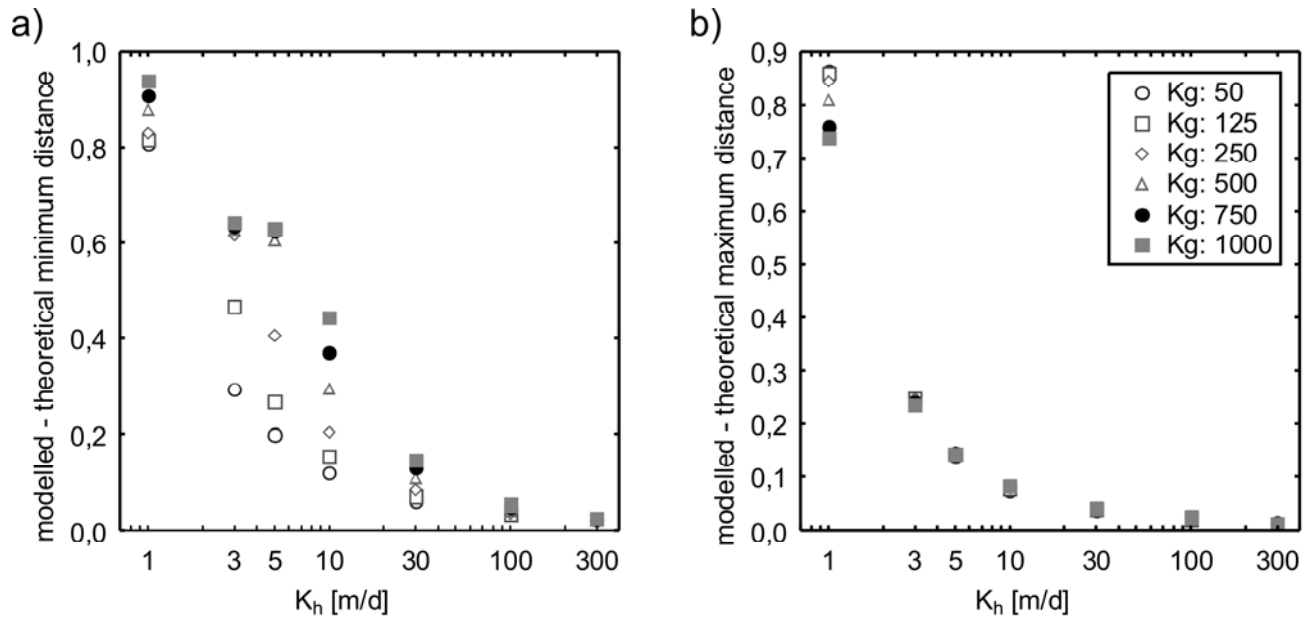
288

289 For further analysis of the capture zone location and size, we separately refer to the width and length
290 of the narrow, “elongated” part of the capture zone nearer to the well and of the “main” part of the
291 capture zone (**Figure 6**) from where the majority of the water originates. The simulations show that
292 the length of the elongated part increases faster than the length of the main part as horizontal aquifer
293 conductivity increases, but the gravel pack conductivity has a significant influence only on the
294 length of the elongated part (**Figure 6c, d**). The same is true for the width of the two capture zone
295 parts: The gravel pack conductivity has a significant influence only on the width of the elongated
296 part but little, yet discernable influence on the main part. The width of the elongated part increases
297 several-fold with gravel pack hydraulic conductivity, K_g , especially in less productive (low K)
298 aquifers. By the same token, the widths of the main and elongated parts (**Figure 6a, b**) decrease
299 with higher aquifer conductivities (more narrow, but longer source area). For low gravel pack
300 conductivities, the width of the elongated part of the capture zone remains nearly constant,
301 regardless of aquifer conductivity



302
 303 **Figure 6:** Widths (top panels) and lengths (bottom panels) of the elongated part (right panels) and
 304 the main part (left panels) of the capture zone for an anisotropy ratio of $K_v : K_h = 1 : 2$. Behavior of
 305 the models with an anisotropy ratio $K_v : K_h = 1 : 5$ is similar.
 306

307 The analytical model (eqs. 2,3) of the source area location provides good approximations of the
 308 source area only in highly permeable aquifers. For aquifers with intermediate and low conductivity,
 309 the gravel pack has significant influence on the distance of the downgradient edge of the capture
 310 zone from the well (**Figure 7a**), where the source area can be as much as 90% closer to the well than
 311 estimated from eq. 2. The analytical approximation of the distance from the well to the upgradient
 312 edge of the source area (eq. 3) is relatively close to the numerical simulations if aquifer hydraulic
 313 conductivities are above 5 m/d. In those cases, the relative difference between analytical and
 314 numerical model is on the order of 10% or less (**Figure 7b**), regardless of anisotropy ratio and gravel
 315 pack hydraulic conductivity.



316
 317 **Figure 7:** Comparison of the distances of the source areas to the well provided by the numerical and
 318 by the analytical model exemplarily for an anisotropy ratio of $K_v: K_h = 1 : 2$. (a) Normalized
 319 differences between the modeled and analytically calculated distances of the downgradient edges of
 320 the source areas to the well. (b) Normalized differences of the distances of the upgradient edges of
 321 the source areas to the well.
 322

323 The simulation results show that water moves downward inside the gravel pack above the well-
 324 screen from considerable distances: For K_h less than 10 m/d and high gravel pack hydraulic
 325 conductivities, water travels downward from as far as the top of the gravel pack, 30 m above the
 326 well-screen (**Figure 8**). Again, the more permeable the gravel pack in the annulus, the larger the
 327 above-screen capture of source water. The fraction of well pumpage that originates from capture in
 328 the gravel pack above the well-screen increases as the aquifer hydraulic conductivity decreases
 329 (**Figure 9**). In intermediate and low permeable aquifers, domestic wells with highly permeable
 330 gravel packs receive from 20% to 50% of the total well flow from the extended gravel pack above
 331 the screened aquifer horizon. This model result is qualitatively consistent with the field data of
 332 Houben (2006), who found iron oxide incrustations in the gravel pack significantly above the top of
 333 the well screen, where the incrustations were due to a significant amount of water flowing through
 334 the upper part of the gravel pack. At high aquifer conductivities ($K_h > 10$ m/d), less than 12 % of the

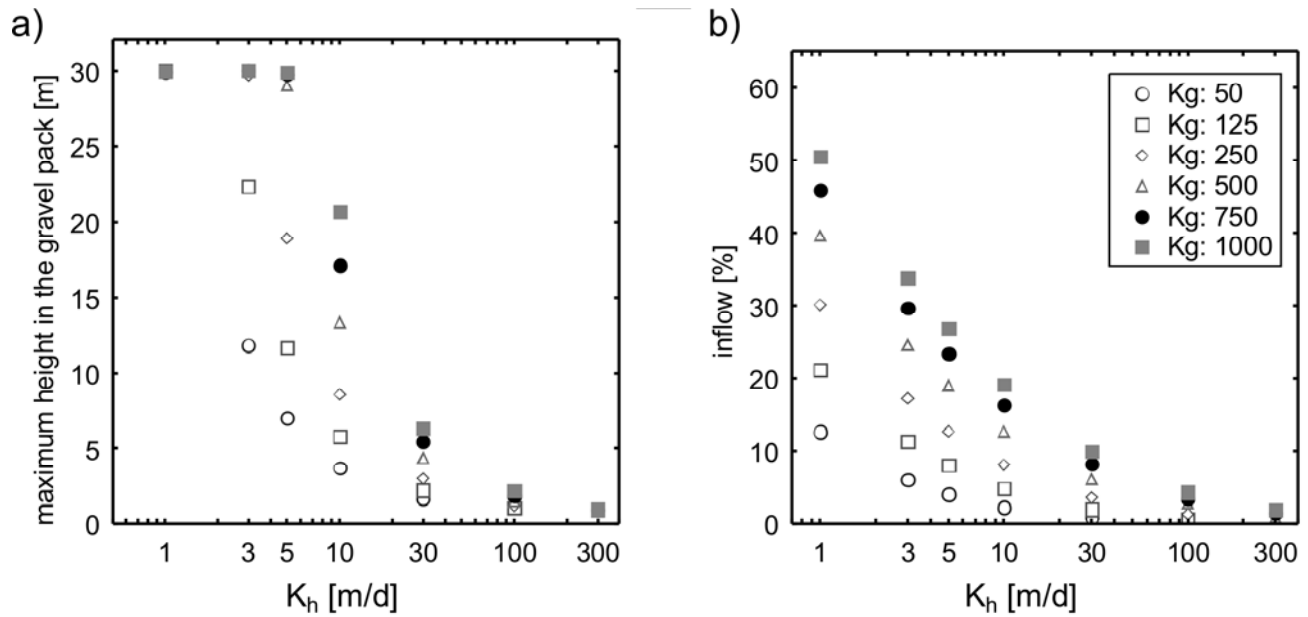
335 total domestic well flow originate from the gravel pack above the well screen. Aquifer anisotropy
336 has little influence on the height of the capture zone within the gravel pack.

337

338 The height of the gravel pack participating in flow to the well and the percent fraction of the
339 pumpage originating from the gravel pack above the screen can be expressed quantitatively: **Table**
340 **2** provides the regression coefficients obtained by fitting data in **Figures 8a and 8b** to nonlinear
341 exponential regression equations of the form:

342
$$y = a * \exp(-\log(K_h)/b) \quad (9)$$

343 using the Levenberg-Marquardt algorithm for optimization. For application to a specific site, linear
344 interpolation of the values for a and b in **Table 2** may be used to compute the height of capture in
345 the gravel pack and the proportion of flow originating from the gravel pack above the well screen for
346 values of the anisotropy ratio and of K_g other than those given in the Table. This modified analytical
347 tool provides a much more realistic source area than the much simpler graphical method employed
348 in many states as part of their source water assessment programs (e.g., California DHS 1999).



349

350 **Figure 8:** (a) Maximum virtual water particle heights in the gravel pack above the well screen
 351 serving to capture water (b) Percentage of inflow into the well screen flowing through the gravel
 352 pack from above the screen. Both for an anisotropy ratio of 2.
 353

354

355

356

Anisotrop y	K_g	Parameter for maximum heights:		Adjusted r^2	Parameter for inflow from above:		Adjusted r^2
		a	b		A	b	
2	50	33.31	1.05	1.00	12.69	0.60	0.99
2	125	77.01	0.88	0.99	21.44	0.69	0.99
2	250	87.95	1.02	1.00	30.59	0.76	0.99
2	500	163.35	0.93	1.00	40.57	0.86	0.99
2	750	172.04	1.00	1.00	47.16	0.92	0.99
2	1000	226.70	0.96	0.94	52.10	0.96	0.98
5	50	79.01	0.78	0.95	14.94	0.61	1.00
5	125	98.28	0.93	0.97	25.14	0.70	0.99
5	250	216.33	0.80	0.93	35.57	0.77	0.99
5	500	276.67	0.87	0.99	47.59	0.85	0.99
5	750	396.12	0.85	0.99	55.54	0.91	0.99
5	1000	401.91	0.88	1.00	61.39	0.96	0.98

357 **Table 2:** Coefficients and adjusted coefficients of determination (r^2) for the equations describing the
 358 maximum heights of the capture zone in the gravel pack, and the inflow of water entering the well
 359 from the gravel pack above the screen.
 360

361

362

363 **Discussion**

364 For application to specific sites, Figure 7 provides a tool to estimate the additional source area due to
365 the gravel pack, when compared to the simple approximation (eq. 2). These results can also be
366 applied for conditions with smaller or larger recharge rates, R' , than the rate $R = 0.669$ m/a used in
367 our computations. For R' not equal to R , results shown in Figures 7-10 and expressed in the above
368 equation are looked up for a scaled hydraulic conductivity K' rather than for the actual hydraulic
369 conductivity K , where $K' = K \cdot R'/R$. This scaling procedure is approximate because it does not
370 simultaneously scale other parameters controlling the observed results, e.g., screen length and
371 pumping rate. However, for applications in unconsolidated sedimentary aquifers, this scaling
372 approach works well as the drawdown created by domestic wells is relatively small. For depths to
373 the top of the screen different from that used here, the simple geometric conceptual model outlined
374 in Figure 1 and expressed in eq. 2 provides a framework for adjusting the distance of the source area
375 from the well head. Equation 9 (with Table 2) can be used to estimate the fraction of flow
376 originating from the elongated part of the source area.

377

378 The numerical modeling shows the significant influence of the gravel pack on the source area of a
379 domestic well, particularly for lower permeable aquifers (horizontal hydraulic conductivities of less
380 than 10 m/d). In highly permeable aquifers (relative to the recharge rate of 0.669 m/year used in this
381 study), the analytical model (eqs. 2, 3) provides a relatively good approximation of the upgradient
382 and downgradient edge of the source area. Lower hydraulic conductivities lead to significantly
383 longer capture zones than predicted by the analytical model (eqs. 2-3). In our configuration of screen
384 length and gravel pack length, which represents an average domestic well construction for Central
385 California, the elongation due to the presence of a gravel pack constitutes up to 70 % of the total

386 length of the capture zone. The elongation is relatively narrow but higher gravel pack conductivities
387 lead to significant increases in that width. The width of the main capture zone, in turn, slightly
388 decreases at higher gravel pack conductivities. The greater the difference between hydraulic
389 conductivity of the aquifer and that of the gravel pack, the greater is the elongated part relative to the
390 total length of the capture zone.

391

392 For many contaminants, chemical or microbial, aquifer attenuation is a dynamic, time-dependent
393 process. Travel times for potential contaminants decrease approximately linearly with increased
394 gravel pack length above the well screen. This is due to the strong influence of recharge on vertical
395 downward displacement of water (and contaminants) and the relatively small influence that the
396 domestic well pumping exerts on the overall groundwater flow field. A linear decrease in travel time
397 from the time of recharge until arrival at the gravel pack is associated with exponentially increased
398 contaminant concentrations. The gravel pack itself typically provides much less attenuation capacity
399 than the aquifer material. Hence, a short seal and vertically extended gravel pack constitute a
400 potential short-circuit for contaminants.

401

402 We also note that the fraction of flow captured by the gravel pack above the well screen may be
403 relatively small in a productive (high K) aquifer. But for some contaminants the resulting dilution
404 with (good) groundwater collected by the well at the depth of the screen may not be sufficient. This
405 includes contaminants that reach the water table at concentrations that are several orders of
406 magnitude above regulatory drinking water limits including solvents, pesticides, other organic
407 chemicals, and pathogens. A possibly common source of such contamination are septic tank leach

408 fields, which - in rural and semi-rural housing developments - are often located in the vicinity of
409 domestic wells.

410

411 **Conclusions**

412 Our work provides a tool to quickly estimate the size and location of the source area of domestic
413 wells in regions with significant recharge (for example, due to irrigation). The influence of the
414 gravel (or sand) pack in the well annulus above the well screen is explicitly accounted for. Results
415 allow for estimation of source area and gravel pack impact for a wide range of scenarios.
416 Importantly, we show that the gravel pack above the well screen poses a significantly increased risk
417 for domestic well contamination. A gravel pack that extends significantly above the well screen (due
418 to short seal length), may significantly enhance the length of the source area, thus exposing the well
419 to a larger cross-section of potential contaminant sources. The extended gravel pack also decreases
420 travel time and distance for contaminants from the source area to the well allowing for contaminants
421 to partially circumvent natural aquifer attenuation. This is especially true in aquifers with low to
422 intermediate hydraulic conductivity ($K \leq 10$ m/d). We therefore strongly recommend that the gravel
423 (or sand) pack not be extended more than a few meters above the well screen of a domestic well.

424

425 **Acknowledgments.** We gratefully acknowledge the careful review and constructive comments of
426 Karen Burow, USGS, and two anonymous reviewers. Funding for this research was provided
427 through a fellowship of the German Academic Exchange Service (DAAD) to Judith Horn.

428

429

430

431 **References**

- 432 Belitz, K., and S. P. Phillips (1995), Alternative to agriculture drains in California's San Joaquin
433 valley: results of a regional-scale hydrogeologic approach, *Water Resour. Res.*, 31(8), 1845-1862.
434
- 435 Burow, K. R., J. L. Shelton, J. A. Hevesi, and G. S. Weissmann. 2004. Hydrogeologic
436 characterization of the Modesto area, San Joaquin Valley, California. USGS Scientific Investigations
437 Report 2004-5232.
438
- 439 California DHS. 1999. Drinking Water Source Assessment and Protection (DWSAP) Program.
440 Division of Drinking Water and Environmental Management, California Department of Health
441 Services. Sacramento, CA. <http://www.dhs.ca.gov/ps/ddwem/dwsap/DWSAPindex.htm>
442
- 443 Garg, S. P. and J. Lal, 1971. Rational design of well screens. *J. Irrig. and Drain. Div.*, ASCE,
444 97(1):24-35.
445
- 446 Harter, T. 2008. Delineation of wellhead protection areas. In: T. Harter and L. Rollins (eds.), 2008.
447 *Watersheds, Groundwater, and Drinking Water: A Practical Guide*, University of California, UC
448 ANR Communications Services Publication 3497, Davis, CA 95616, 274p.
449
- 450 Houben, G. H. 2006. The influence of well hydraulics on the spatial distribution of well
451 incrustations. *Ground Water* 44, no. 4: 668-675.
452
- 453 McCray, J. E., S. L. Kirkland, R. L. Siegrist, and G. D. Thyne. 2005. Model parameters for
454 simulating fate and transport of on-site wastewater nutrients. *Ground Water* 43, no. 4: 628-629.
455
- 456 McDonald, M. G. and A. W. Harbaugh. 1988. Technics of water-resources investigation of the
457 United States Geological Survey. USGS Open-File Report 83-875.
458
- 459 Nahrgang, G., 1954. Zur Theorie des vollkommenen und unvollkommenen Brunnens. 43 p.
460
- 461 Phillips, S. P., C. T. Green, K. R. Burow, J. L. Shelton, and D. L. Rewis, 2007. Simulation of
462 ground-water flow in part of the Northeastern San Joaquin Valley, California, U.S. Geological
463 Survey, Scientific Investigations Report, SIR 2007-5009.
464
- 465 Pollock, D. W. 1994. User's guide for MODPATH/MODPATH-PLOT, Version 3: A particle
466 tracking post-processing package for MODFLOW, the U. S. Geological Survey finite-difference
467 ground-water flow model. USGS Open-File Report 94-464.
468
- 469 Todd, D. K. 1980. *Ground water hydrology*, 2nd ed. New York: John Wiley and Sons.
470
- 471 U.S. EPA. 1997. Response to Congress on use of decentralized wastewater treatment systems.
472 Washington, D.C.: Office of Water, U.S. EPA.
473
- 474 VonHofe, F. and O. J. Helweg, 1998. Modeling well hydrodynamics. *ASCE J. Hydr. Eng.*
475 124(12):1198-1202.

